Archaeological Prospection
Archaeol. Prospect. **9**, 135–156 (2002)
Published online 12 April 2002 in Wiley InterScience (www.interscience.wiley.com). DOI: 10.1002/arp.183

Georadar in the Roman Civil Town Carnuntum, Austria: An Approach for Archaeological Interpretation of GPR Data

W. NEUBAUER,[1,2]* A. EDER-HINTERLEITNER,[2] S. SEREN[2] AND P. MELICHAR[2]

[1] *Vienna Institute for Archaeological Science, University of Vienna, Franz Kleingasse 1/V, A-1190 Vienna, Austria*
[2] *Archeo Prospections, Central Institute for Meteorology and Geodynamics, Department for Geophysics, Hohe Warte 38, A-1190 Vienna, Austria*

ABSTRACT The case study presented is a prime example of integrated geophysical–archaeological prospection. The aerial photographs available are complemented by non-destructive geomagnetic and geoelectric surveys with a reading distance of 0.5 m or less. To gain depth information and provide higher resolution, ground-penetrating radar (GPR) data are integrated. The GPR data were collected in a 0.5×0.05 m raster and visualized as black-and-white time or depth slices. The developments presented allow us to incorporate GPR into the standardized interpretation process of archaeological prospection based on a geographical information system (Grs). Using GPR and all the other prospection data available as a basis, a detailed three-dimensional interpretation model of the monument detected, the southern part of the forum of the civil town of Roman Carnuntum, is created.

Key words: GPR; integrated archaeological prospection; archaeological interpretation; GIS

Introduction

Archaeological geophysical prospection

Geophysical prospection has become an important archaeological discipline featuring geomagnetic and geoelectrical methods. Archaeological applications demand specific measurement devices and configurations for rapid coverage of large areas (>1 ha). Only surveying with the highest resolution measuring devices in small raster (≤0.5 m) is the guarantee for detecting even smallest structures of archaeological interest (postholes, palisades, etc.). In particular, geomagnetic prospection, using caesium multisensor gradiometers, developed into a very fast method of great archaeological interest enabling the survey of more than 4 ha daily in 0.125×0.5 m raster with an accuracy of a few picotesla (Becker, 1995; Neubauer *et al.*, 1996, in press). Geomagnetic prospection became a high speed technique (Neubauer, 2001b) giving the opportunity to cover areas 10 times as large as with any other technique in the same time (Table 1). Geoelectrical prospection in the way of resistivity mapping, using Geoscan RM15 equipment, seems to have become an archaeological standard (Clark, 1990; Walker, 2000). The large amount of data collected in geophysical archaeological prospection can be processed and visualized with specific software. The aim of such processing is to

* Correspondence to: W. Neubauer, Vienna Institute for Archaeological Science, University of Vienna, Franz Kleingasse 1/V, A-1190 Vienna, Austria.
E-mail: wolfgang.neubauer@univie.ac.at

Received 1 June 2001
Accepted 19 December 2001

Table 1. Comparison of prospectable area with specific spatial resolution in 8 h and main archaeological features producing good response

Method and instrument	Time (h)	Area (m^2)	Resolution (m)	Main features
Geomagnetic survey EP750 multisensor Cs-gradiometer	8	50 000	0.125 × 0.5	Pits, ditches, bricks, tiles, iron objects, burned clay, posts
Resistivity surveying RM15 Twin Array, MPX5 probe separation 0.5 and 1.0 m	8	5000	0.5 × 0.5 0.5 × 1.0	Stone walls, floors, stony areas, streets
GPR survey PulseEKKO 1000	8	5000	0.05 × 0.5	Stone walls, floors, stony areas, streets, basements, stairs, voids, main stratigraphy

visualize comprehensive representations of the data for subsequent archaeological interpretation. Digital image representations proved to be the most suitable for visualization of magnetic and resistivity data, enabling cognitive perception of archaeological structures even by lay people (Becker, 1985; Scollar *et al*., 1986; Neubauer 1990; Neubauer *et al*., 1996; Neubauer, 2001a).

As can be shown by comparative studies, ground-penetrating radar (GPR) responds to similar physical properties of the near surface as resistivity mapping does and thus is able to locate the same groups of archaeological structures but with far more detail and with a higher accuracy in the same measuring time (Table 1). The higher resolution and the possibility to derive depth information from the data would favour GPR for archaeological applications, but the time needed so far for data processing and deriving an archaeologically relevant interpretation has reduced its worth and made it an expensive way of non-destructive evaluation of archaeological information.

The case study

This paper and a recently published one on combined interpretation of prospection data (Neubauer and Eder-Hinterleitner, 1997), summarize the results of a research project funded by the Austrian Ministry of Science and Traffic carried out in 1998. The aim of the project was the development of standardized methods for combined archaeological geophysical prospection towards a detailed archaeological interpretation model. As a case study for a combined application of aerial photography, geomagnetics, resisitivity and GPR, the Roman town Carnuntum east of Vienna (Jobst, 1983) was selected. A total area of more than 450 h a within the communities of Petronell and Bad Deutsch Altenburg can be classified as an archaeological area, of which only a small part of the archaeologically has been dealt with so far. A complete inventory of all available aerial photographs will be compiled soon (Doneus *et al*., 2001). Interpretation of aerial photographs using digital photogrammetry provides a first accurate overview of the archaeological structures visible over the past decades and will be reported in a following paper.

Parts of the area had been prospected successfully applying geomagnetic and/or geoelectrical methods. The aerial photographs and the existing geophysical data show an increasing degree of severe destruction of the heritage by deep ploughing. This deep ploughing sometimes is initiated by 'hobby archaeologists' and turns even walls and floors up to the surface for easy systematic robbery with metal detectors. As constant excavation and reconstruction work is done in the archaeological park of Carnuntum, much unforeseen rescue excavation had to be done owing to various building activities, often ending in long-term projects. Scientific interests frequently are in conflict with the economic and housing development of the present-day villages of Petronell and Bad Deutsch Altenburg, situated right in the archaeological zone. Thus the working out of an appropriate prospection strategy applying non-intrusive methods for Carnuntum, the largest archaeological landscape in Austria, seems to be an important step for further archaeological research and monument protection as well as regional planning.

To demonstrate the high potential of combined prospection we selected the recently detected and already presented building complex in the civil town (Neubauer and Eder-Hinterleitner, 1997). It shows three major halls forming the southern part of the forum, detected by resisitivity surveying (Figure 1). North of the forum the monumental public bath 'Große Therme' is situated. The geoelectrical and geomagnetic surveys are already reported and their combined archaeological interpretation should be complemented by a GPR survey covering the same 80×80 m area and providing depth information and more details on the interesting building complex. The GPR data should be combined with magnetics and resisitivity data on the same digital image visualization and interpretation standards based on a geographical information system (GIS) and developed during the past 10 years. We tried to form a three-dimensional archaeological interpretation model as detailed as possible and to visualize it in a comprehensive way.

Archaeological application of GPR

Although magnetic and geoelectrical methods are widely accepted and more and more often applied, the archaeological application of GPR still suffers from unsuitable survey logistics, data processing, visualization and interpretation

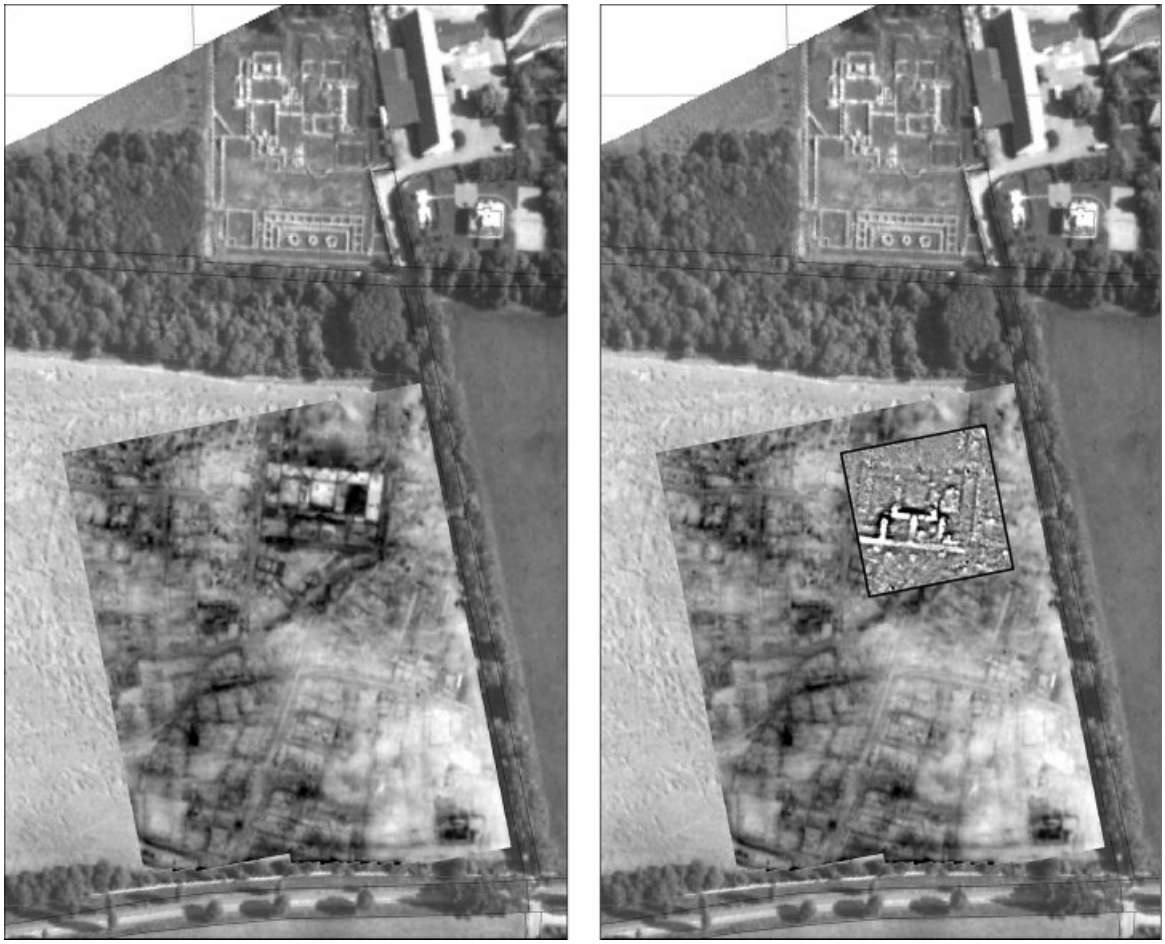

Figure 1. Orthophotograph superimposed with the result of the resistivity survey (left) and by the result of the resistivity and magnetic survey (right). The excavated monumental public bath 'Groβe Therme' is visible at the top on both sides. The area of the magnetic survey (80 m $\times$ 80 m) is selected for the GPR case study. Resistivity: twin array, $a = 0.5$ m, 80–180 Ωm. Magnetic: gradient 0.5/2.0 m, -5 to 10 nT. Orthophotograph release number: BMLV Nr.: 13.088/12-1.4/00.

techniques. The theoretically high archaeological potential of the method has not been convincingly presented to the archaeologists so far. Ground penetrating radar produces a large amount of data with high information density. Visualization of data is done mainly in black and white or colour coded representations of received amplitudes by time and distance in single sections known as a 'radargram' (Figure 2). These representations of single sections show typical diffraction and reflection patterns that are not easily understandable. One could even assume that it is nearly impossible for inexperienced archaeologists to interpret anything in such a radargram. For that reason GPR operators usually line out anomalies or add annotations to the radargram to enable visual perception of the main structures. This manual 'image enhancing' technique mainly uses the single GPR sections. By comparison of the various sections the interpreter tries to line out correlating diffraction and reflection patterns and to assign these to (mostly known) archaeological structures. The anomalies detected within the sections can then be shown in an anomaly map, representing the three-dimensional information compiled in a two-dimensional map. Depth information is—if at all-mainly added only punctually for single structures. The result of such an interpretation depends very much on the complexity of the stratification of the site, the knowledge and archaeological experience of the interpreter and the time available for data analysis, and is thus hard to reproduce and to evaluate. Such a reduced two-dimensional interpretation uses only a small part of the information inherent to GPR data and these interpretation techniques are definitely not suitable to line out weak anomalies or the depth of archaeological features.

Therefore, despite some positive results in small-scale applications and case studies, most of the GPR surveys presented so far have shown disillusioning results from an archaeological point of view and even brought GPR a rather negative feedback from archaeologists. The intensive methodological research and development in close cooperation with archaeology marking the early years of archaeological geoelectrics and geomagnetics was not done sufficiently on archaeological GPR. Not even the high interest shown by archaeologists, various test programmes and development requests could then invoke an appropriate development for GPR hardware and software by the production companies because the 'market was not large enough'. The development of hardware and software and the standardization of the application, data collection, presentation and interpretation recently has been proposed (McCann, 1995) and could

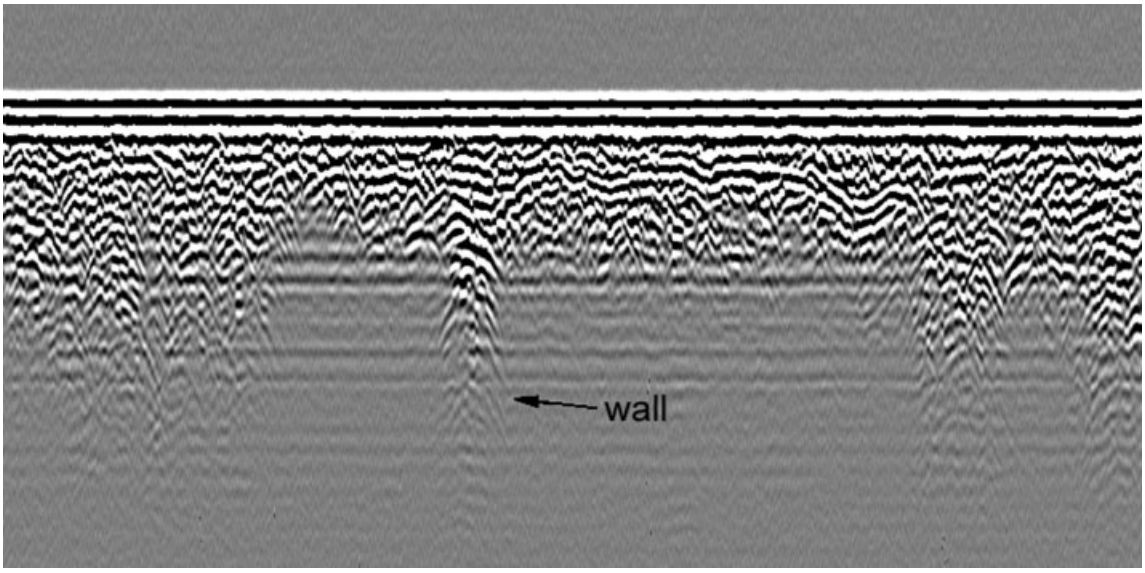

Figure 2. Conventional radargram with a marked anomaly produced by a known wall from the GPR case study at Carnuntum. Section length 40 m; number of traces 801; time window 80 ns.

be a first step to establish GPR in archaeological research. To use the high archaeological potential of this method new techniques of processing are necessary for producing objective and reproducible results (Goodman, 1994; Conyers and Goodmann, 1997). One of these techniques is the use of horizontal time slices as regular GPR data representations (Goodman *et al*., 1995; Lorra, 1996; Malagodi *et al*., 1996). Such a time slice is created by calculating the reflected energy of the radar waves within a certain time window Δt at any discrete reading (x,y) of the regular or irregular measurement grid. The reflected energy is calculated by summing up the absolute amplitudes of the digitized wave $a(x,y,t)$ within the time window Δt. We consequently propose here the use of a three-dimensional data block $A(x,y,z)$ of amplitudes, where x and y represent the measured grid and z the number of the calculated time slice

$$A(x, y, z) = \sum_{t=z^*\Delta t}^{(z+1)^*\Delta t} |a(x, y, t)|$$

As the scope of the research project reported here is a standardization of a combined geophysical approach towards a detailed archaeological interpretation model, the application of GPR made some basic research necessary. As a first step we had to find the appropriate configuration and measurement parameters for successful archaeological fieldwork. Therefore we carried out some test measurements, and in a second step, developed processing, visualization and interpretation techniques to include georadar into the GIS-based archaeological interpretation process. The third step was the integrated archaeological interpretation and the working out of a three-dimensional interpretation model.

Configuration and measurement parameters

There are a number of different GPR systems used in archaeology. Most of them transmit pulsed radar energy of one centre frequency. Most of the published GPR applications in archaeology were carried out with antennae having a centre frequency of 200–1000 MHz depending on site parameters and the archaeological problem to be solved. All recent work is done by using digital GPR units. The surveys were done either with discrete inline reading to a reading distance of 0.02 to 0.5 m or with continuous sampling on profiles 1 to 5 m apart, resulting in a series of radar sections.

To define the adequate measurement parameters, survey logistics and configuration, a 20 × 40 m test area was selected and various measurements were carried out using a digital PulseEKKO 1000 device with 16 bit resolution and 96 dB dynamic range and sampling rates of 10 to 20000 ps (Figure 3).

Choice of antenna

The wave length of an electromagnetic signal defines the lateral and vertical resolution. In practice a resolution of interfaces or objects with a vertical distance equal to or larger than half the wave length is feasible. The horizontal resolution, however, depends on the frequency, the signal velocity, the reflector–antenna distance and the radiation characteristics of the antenna. Resolution is proportional to the frequency and inversely proportional to penetration depth. Therefore to reach greater penetration depths lower frequencies should be used, for higher resolution, higher frequencies are recommended. In practice a compromise depending on the given problem is advisable. Usually test measurements with different frequencies lead to a satisfactory middle course. In the case study presented in this paper two antennae with 450 MHz and 225 MHz respectively were tested, the 450 MHz antenna qualifying for the measurements. The penetration depth of the 450 MHz antenna was deep enough.

Line distance and reading distance

To determine the necessary density of readings the test area was measured with 0.5 m line distance and in an inline distance of 0.05 m. By reducing the data set, further densities, as is obvious from Table 2, were simulated. To visualize the effect of the various densities the 30 to 31.5 ns time slice in grey scale digital image representation was used (Figure 4).

As is obvious in Figure 4c, f and i, measurements with 2 m line distance—independent of

Figure 3. The GPR system PulseEKKO 1000 equipped with 450 MHz antennae and odometer during measurement at the Roman town of Carnuntum in winter 1998. The parallel measuring lines have a distance of 50 cm.

Table 2. Geological and mineralogical comment on the change of the amplitudes with depth

Depth range (m)	Amplitude ratio (%)	Geological and mineralogical comment
0.0–0.15/0.15–0.30	52	Humus, Ap horizon
0.15–0.30/0.30–0.45	−79	Humus, Ap horizon
0.30–0.45/0.45–0.60	−49	Humus, Ap horizon
0.45–0.60/0.60–0.75	−38	Clayey
0.60–0.75/0.75–0.90	−37	Clayey
0.75–0.90/0.90–1.05	−33	Clayey/sandy
0.90–1.05/1.05–1.20	−31	Clayey/sandy
1.05–1.20/1.20–1.35	−28	Clayey/sandy
1.20–1.35/1.35–1.50	−26	Clayey/sandy
1.35–1.50/1.50–1.65	−30	Clayey/sandy
1.50–1.65/1.65–1.80	−26	Sandy/silty
1.65–1.80/1.80–1.95	−25	Sandy/silty
1.80–1.95/1.95–2.10	−17	Sandy
1.95–2.10/2.10–2.25	−17	Sandy
2.10–2.25/2.25–2.40	−5	Sand/gravel
2.25–2.40/2.40–2.55	−9	Sand/gravel
2.40–2.55/2.55–2.70	−7	Sand/gravel
2.55–2.70/2.70–2.85	−4	Sand/gravel
2.70–2.85/2.85–3.00	−3	Sand/gravel
3.85–3.00/3.00–3.15	−1	Sand/gravel
3.00–3.15/3.15–3.30	−1	Sand/gravel

the inline reading distance-cannot be interpreted correctly archaeologically as all structures are completely lost. Also measurements with 1 m line distance (Figure 4b, e and h) are not correctly interpretable: several walls appear interrupted and superficial features are introduced by the necessary interpolation. Only measurements with 0.5 m line distance are archaeologically relevant. The visualization with 0.2 m reading distance (Figure 4g) appears distinctly blurred whereas the 0.05 and 0.1 m reading distances supply sharper images, showing slight but negligible differences. We can conclude that for archaeological GPR applications, such as locating walls, the line distance has to be 0.5 m or less and the inline reading distance should not exceed 0.1 m. An inline reading distance of 0.05 m shows a sharpening effect and offers more flexibility for filtering and further processing such as migration. It has to be underlined that the evidence for these distances is deduced from walls of 1.5 m thickness and with high physical contrast to the

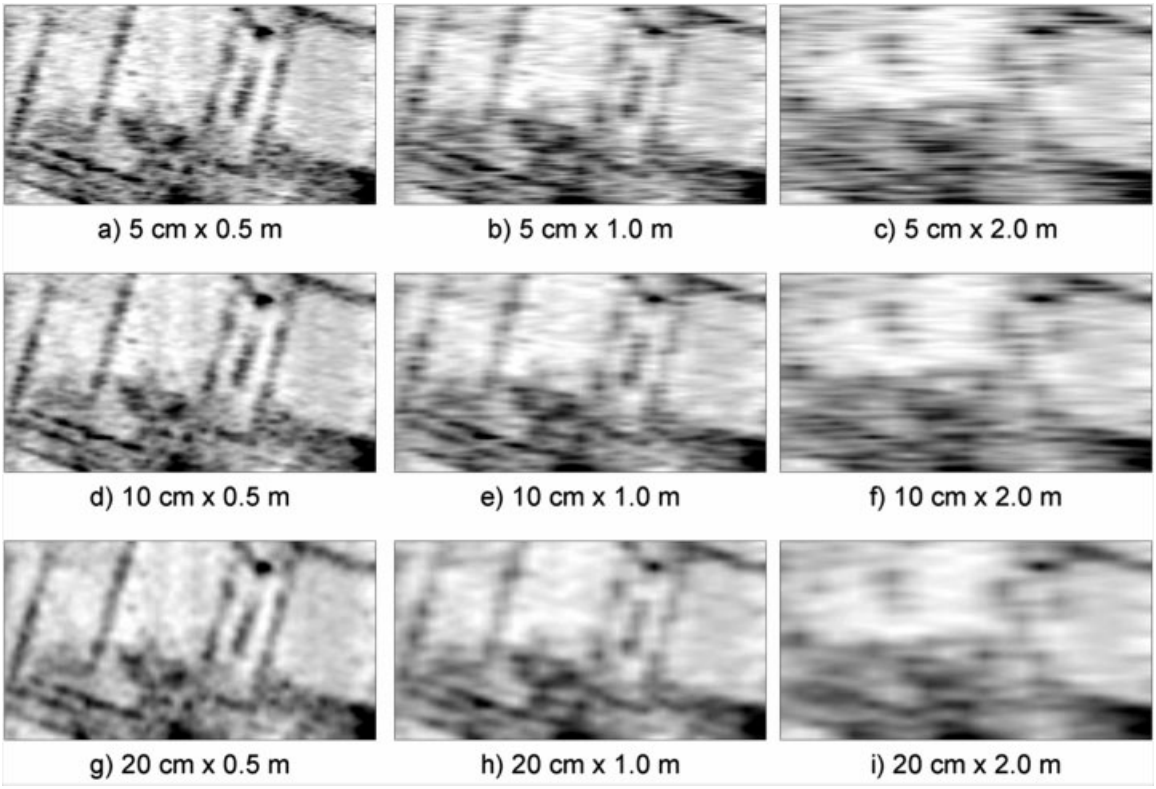

Figure 4. Comparison of different spatial measuring grids. Time slice 30–31.5 ns.

surrounding material. Thinner walls, less contrast or more complex stratification, as is normal in urban archaeology, may require a smaller line distance of 0.25 m, for example.

Orientation of measurement

To answer the question how the orientation of measurement affects the result the test area has been measured again perpendicular to the first. Figure 5 shows the 30 to 31.5 ns time slice measured with 0.5 m line distance and 0.05 m inline reading distance in the y direction (a), in the x direction (b) and in both directions (c). In Figure 5b walls running from bottom to top are better visible than in Figure 5a, whereas walls running from left to right appear more clearly in Figure 5a. The walls are better resolved when the radar sections run perpendicular. Measuring in both directions thus shows the best results for the building but doubles the measuring effort. To define the least time-consuming procedure, giving the best possible results within minimum time, a data set with 1.0 m line distance and 0.05 m inline reading distance in both directions was extracted and compared (Figure 5d). It is obvious that the measurement in only one direction but with half the line distance results in a clearer and more detailed image.

Selected configuration

The final survey was carried out on 6400 m^2 using the 450 MHz antenna on lines 0.5 m apart. The southwestern corner of the area was measured on a rough and wet ploughed surface whereas other parts were measured on a layer of snow 5–10 cm thick. The inline distance on the snow was 0.05 m, on the ploughed field we had to reduce it to 0.2 m. The reflected wave was digitally recorded within a time window of 100 ns using a scanning interval of 0.2 ns and a stacking of two or four. We carried out CMP (Common Mid Point) measurements to determine a mean propagation velocity of 0.1 m ns^{-1}.

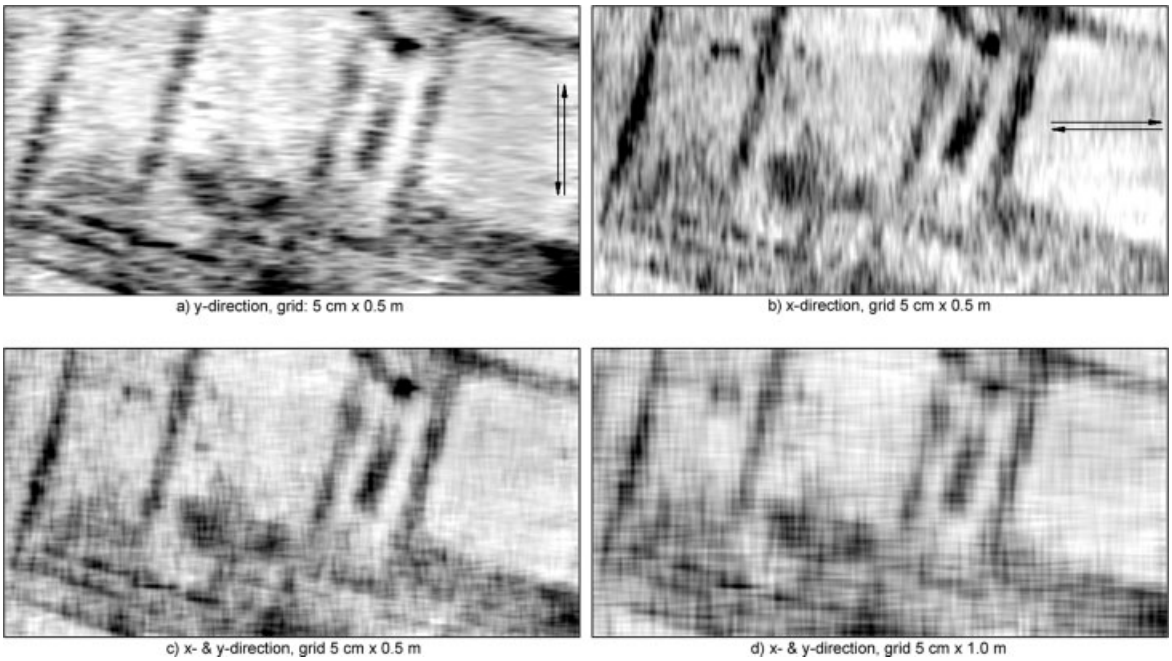

Figure 5. Comparison of different directions of measurement and combination of both directions with different measuring grids. The walls are better resolved when the radar sections run perpendicular. Time slice 30–31.5 ns.

Data processing, visualization and interpretation techniques

Amplitude slice maps and three-dimensional image processing

The amplitudes of the reflected waves are the result of changes in the subsurface. The higher the contrasting permittivity at an archaeological layer or feature interface the greater the reflected energy. The analysis of high amplitudes at specific depths defines archaeological features as walls or major layer interfaces. The distribution of the amplitudes within a specified time-window is called a time slice, which provides the possibility of analysing amplitudinal changes within a certain depth. If the observed amplitude changes can be related to archaeological features and the main units of stratification at specific depths by interpretation, they may be used to reconstruct the subsurface in three dimensions. All time slices deduced from the raw data collected in single lines form a three-dimensional data block representing amplitudinal information of the part of the subsurface explored (Figure 6). Out of this data block amplitude anomaly maps may be sliced in horizontal, vertical or any desired grid direction and thickness (see Figure 9). Such amplitude slice maps are used as a base for archaeological interpretation of GPR data as they make it possible to identify the size, shape, location and depth of the buried archaeological structures and the related stratification.

The digital processing of the sections recorded

The digital processing of the sections recorded and the calculation of the three-dimensional data block is completely automated and can be carried out in the field using a laptop computer immediately after finishing a survey. Therefore a standardized measuring technique and specific software were developed to survey areas of arbitrary shape and to ensure data processing without any further interaction. The software developed *APRadar* (Archeo Prospections®) automatically performs all necessary pre-processing of data and calculates time or depth slices. The pre-processing of the data includes the removing of errors, high and low frequencies, drifts, erroneous traces and points and the automatic detection of the time-zero point for each

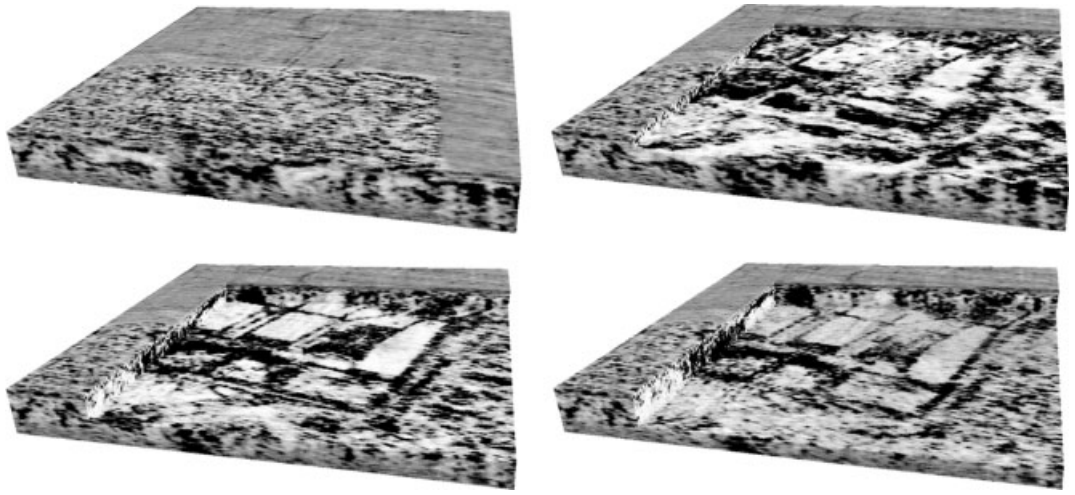

Figure 6. Three-dimensional data block of time slices of reflected energy and three visualizations with excavated parts. Areas with high reflection energy are visualized in black.

single trace. The effect of energy loss with depth is reduced by multiplicative equalization of the slices means. All time slices are given the same mean and therefore can be visualized using the same data range for grey scale representations.

The time slices calculated from pre-processed raw data are combined on a three-dimensional data block and can be processed by further various automatic data enhancement algorithms (Figure 7).

(i) The amplitudes of the time slices are represented non-linearly by computing the square root or the logarithm. Thus small changes in amplitudes are enhanced and details are better visible in the subsequent visualisation (Figure 7b).
(ii) To reduce stripy patterns, small amplitude line shifts in measurement direction caused by small errors in starting time correction or small drifts after breaks, the amplitudes are balanced using the neighbouring lines or by adjusting them to the mean of the time slice (Figure 7c).
(iii) Filtering in the measurement direction by using neighbouring lines is used for smoothing the amplitude information. The filter has to be selected carefully so as not to blur the amplitude information (Figure 7d).

Explorative data analysis

For analysis the three-dimensional data block is imported into the scientific visualization program AVS (Advanced Visual System). The data block is rendered using black-and-white or colour lookup tables. The three-dimensional block can be cut through specifying a plane or particular parts of it can be cut out using the function *excavate* of AVS (Figure 6). Rotation, tilting and shifting, as well as zooming in, allow the archaeologist to explore the data and even animate different pathways through the block. As high-resolution surveys produce large amounts of data the necessity to keep the whole data block in memory can dramatically reduce the response time of the workstation. To reduce the storage consumption we extract two-dimensional images by slicing the data block horizontally or vertically. It is possible to compile various time windows out of the data block into one image to make interpretation more simple. The images derived dynamically from the data block are visualized with commercially available software. We usually produce different stacks of equidistant images in the x, y or z direction, which then can be used for movies. Such an image sequence can be animated forward or backward by varying the speed. This kind of data visualization is very helpful to develop a mental three-dimensional image of the archaeologically relevant structures visible in the data. This mental image helps the observer

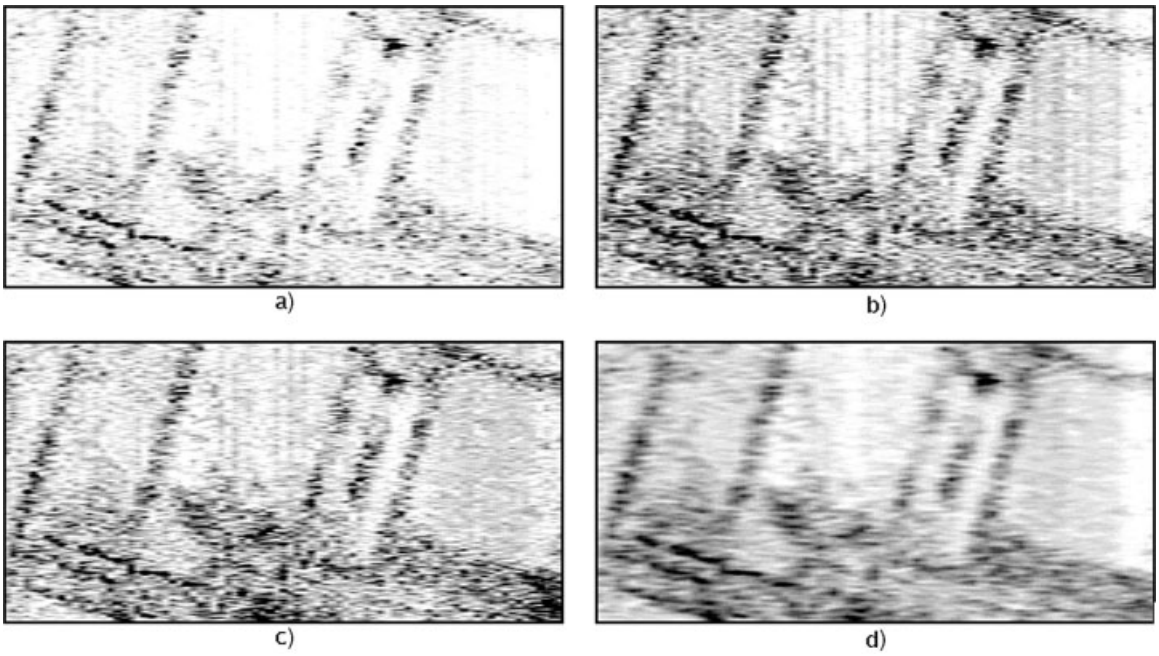

Figure 7. Comparison of different image processing steps: (a) without any image processing; (b) square root of the absolute amplitude; (c) as in (b) plus equalizing line shifts; (d) as in (c) plus 5 × 1 mean filter in measuring direction and 3 × 3 mean filter. Time slice 30–31.5 ns.

not to lose the orientation and the continuity of structures during the graphical interpretation of the sequence of depth or time slices.

Georeferencing and combination

Extended sites usually are prospected in many small areas. They can be combined automatically to one three-dimensional data block and can be transformed into a global co-ordinate system (geo-referencing) using the global co-ordinates of at least four geodetic measured points. The digital images of the time-slices can be produced by *APRadar* to be visualized directly in the G/S *ArcView* for archaeological interpretation (Figure 8). Thus the local co-ordinates of the measurement grid are transformed and any further step of interpretation is done in global co-ordinates.

Comparison of magnetic, resistivity and GPR prospection

The comparison of the results of all three prospection methods clearly shows their different characteristics (Figure 9) and illustrates the potential of the combined archaeological interpretation. Obviously, the magnetic prospection result is completely different from all the others and thus it delivers completely different information for the interpretation process. The GPR prospection result is well comparable to the resistivity measurement because the same geophysical properties are important. However, GPR delivers much sharper results and many more details; it also supplies three-dimensional information. As explained in the section on archaeological interpretation, the information content of all three prospection methods together is more then the sum of the information content in the single methods.

Archaeological interpretation

Identification of archaeologically relevant anomalies is the first step in archaeological interpretation of prospection data. Identification means the demarcation of areas with, for example, high resistivity contrast, higher or low magnetization, high reflectivity, etc. and marking positions of local anomalies. The further interpretation

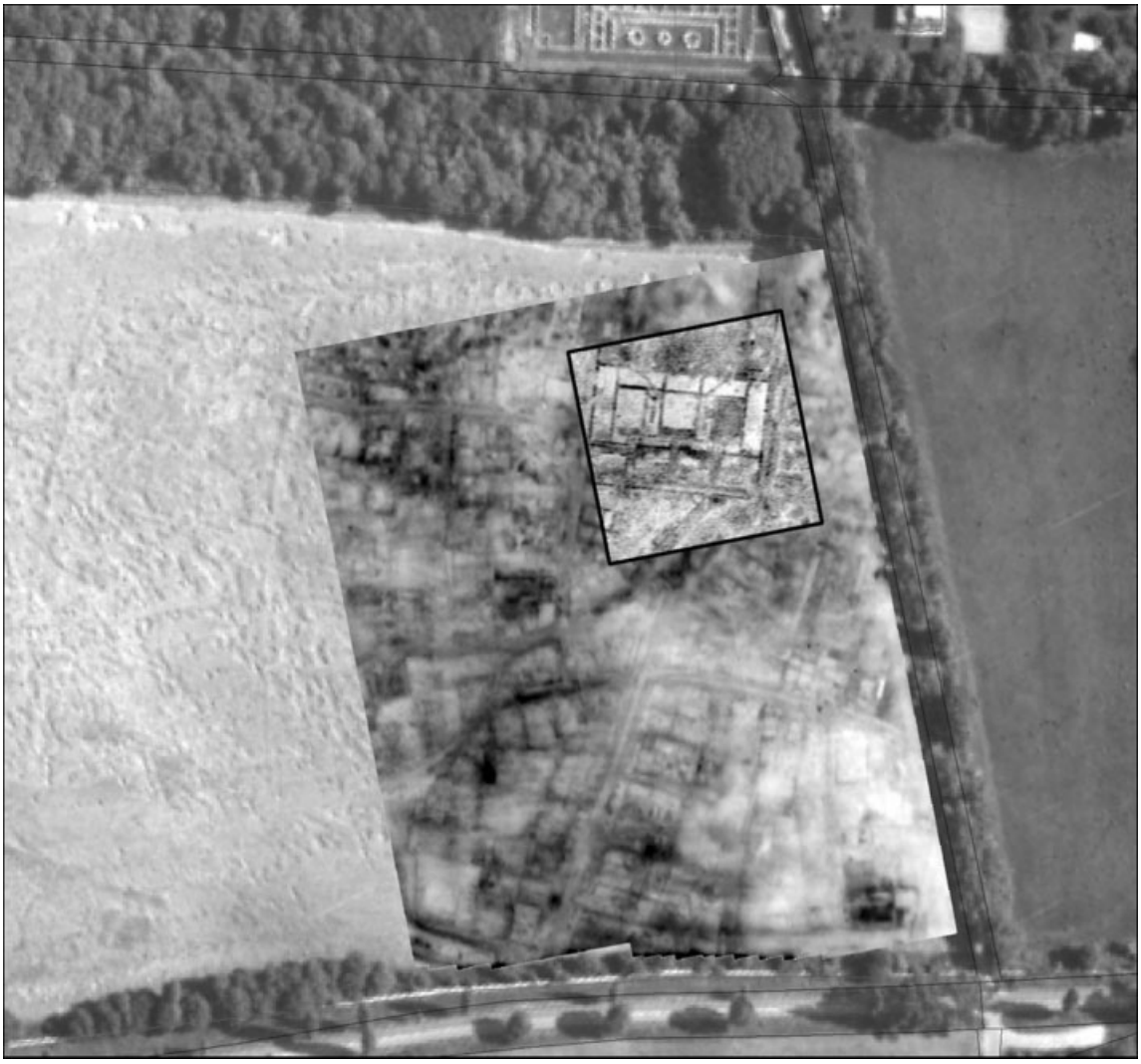

Figure 8. Orthophotograph superimposed with the result of the resistivity and the GPR survey. Resistivity: twin array, $a = 0.5$ m, 80–180 Ωm. GPR: depth slice 1.0 m –2.0 m. Areas with high reflection energy are visualized in black. Orthophotograph release number: BMLV Nr.: 13.088/12-1.4/00.

process is based upon the experience and knowledge of the interpreter, who extracts archaeological structures by mental comparison of recognized anomalies and structures known from excavations. The anomalies or anomalous zones recognized in the first step are thus becoming archaeologically meaningful. The geophysical record is interpreted in the way of an archaeological analysis. Areas of high resistivity contrast can become pavements or streets, linear anomalies the traces of buildings or ditches, local magnetic anomalies are divided into pits, burnt clay structures, fireplaces, postholes or iron debris depending on the pre-information of the site and archaeological experience. Archaeological interpretation therefore is not the marking of anomalous zones or bodies but the non-destructive extraction of archaeological information in the way of producing accurate maps and verbal descriptions and should be done by archaeologists with extended geophysical background in close co-operation with other specialised archaeologists. Accurate maps have to be in the national co-ordinate system, should include all relevant geographical information (e.g. topography, geology, hydrology, cadastral map, etc.), relevant

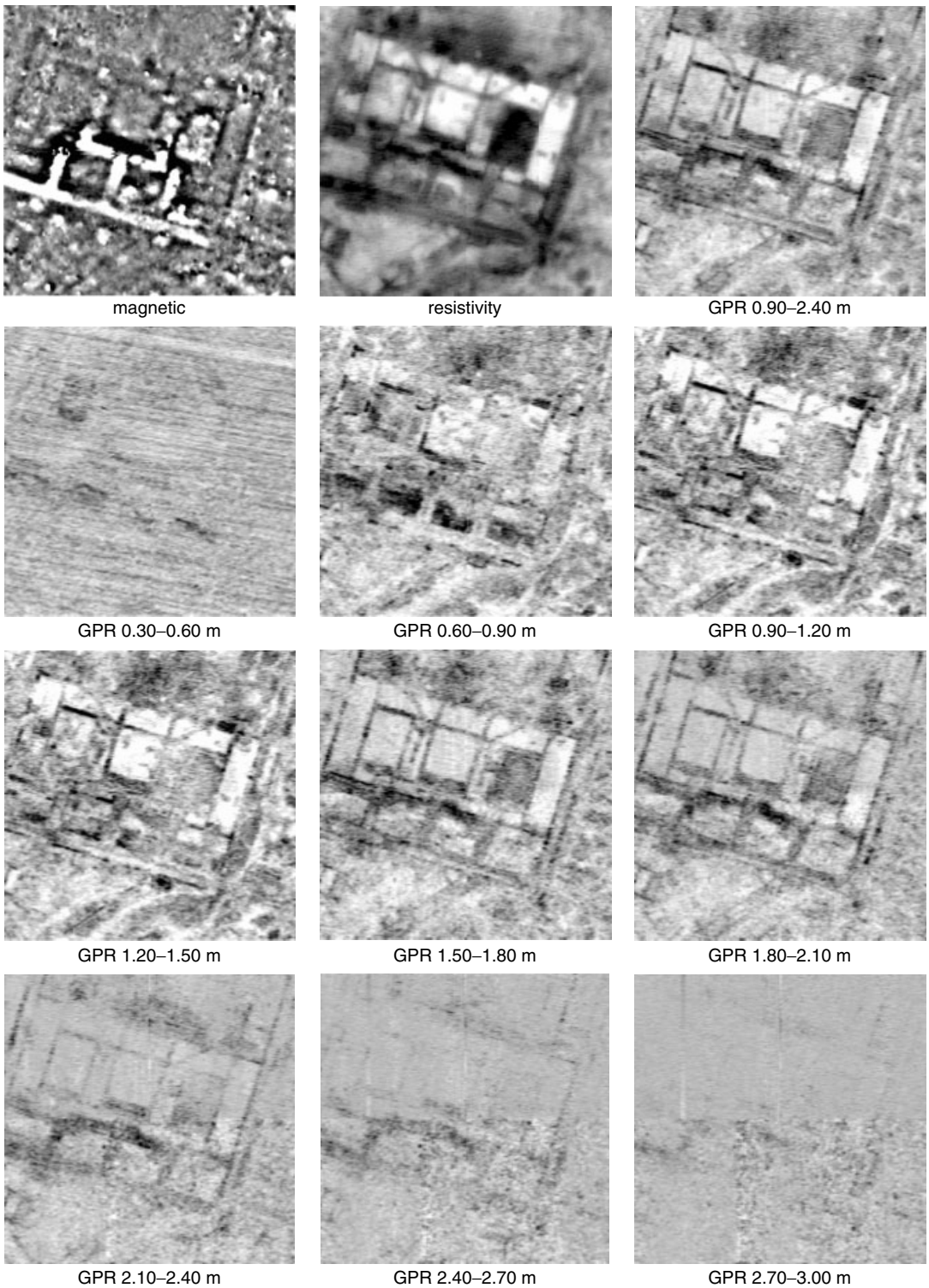

Figure 9. Comparison of the results and information content of different prospecting methods of the same prospecting area of 6400 m^2. Magnetic: gradient 0.5/2.0 m, −5 to 10 nT. Resistivity: twin array, $a = 0.5$ m, 80–180 Ωm. GPR: depth slices of absolute amplitudes, areas with high reflection energy are visualized in black.

archaeological information (excavation trenches, known archaeology, etc.) and the thematically structured interpretative graphic. The graphical content should be clarified by a legend and the interpretation map should be accompanied by a plot of raw data for comparison, preferably using the same scale and not exceeding 1 : 1000. The GIS technology, capable of linking description information with features on the map, is accurate for meeting this demand (Doneus and Neubauer, 1998; Neubauer, 2001b).

Results and archaeological interpretation

Combined interpretation of geoelectric and geomagnetic data

A first preliminary combined interpretation of geoelectric and geomagnetic data for the case study of Carnuntum was published recently (Neubauer and Eder-Hinterleitner, 1997) and will be presented here in an extended version (see Figure 12). We will follow the numbering of the various rooms introduced in that paper. The dimensions were measured from the middle of the walls. The high resolution of the GPR survey makes it possible to be more precise in the room dimensions in the following summary of the main evidence.

The building complex, with more than 3000 m^2 base, is situated at the southern side of a large open square. The dimensions of 66 m in length and 45 m width, together with the wall thickness of 1.5 to 1.6 m and the symmetric layout, indicate an important public building of the civil town of Carnuntum. During the survey the open square north of this complex, recorded so far for a length of 45 m, showed a width of 36 m, flanked by porticoed large halls. The halls comprising smaller rooms are 10 m wide with a 5 m wide porticus facing the open square. The structures found can be interpreted as the southern part of the forum of the civil town, undiscovered for over a century and detected by geophysical prospection. On its northern side the insula with the forum is bordered by the main street, the *decumanus maximus* and the facing complex of the so-called 'Groβe Therme', its maximum extension therefore being 66 × 140 m. The halls with their small units can be regarded as *tabernae*, rows of shops ending in the large, surveyed building complex, allowing the interpretation of a close connection of these buildings. Resistivity anomalies towards the square indicate a staircase leading up to the tripartite front of the large building complex with room C1 apparently serving as entrance hall. Rooms C3 and C4 situated to the left and right symmetrically are cut diagonally by wall-like structures, interpreted as channels or drains. Subsequent to the entrance hall C1, a square room C2 is situated, ending in an oblong, transversal room or platform C5, 3.5 to 4 m broad. The front towards the square was dominated by the three large halls C9, C2 and C10 (150 m^2 each) separated by two long quadrangular corridors C7 and C8 where the above-mentioned channels/drains seem to end. The drains may have been constructed to draw off the rainwater coming down from the roofs. Unlike the western room C9, the eastern C10 shows evidence of paving or a stone floor in the resistivity mapping, as well as a hint of hypocausts in magnetic data. Rooms C9 and C10 are interpreted as assembly rooms, C10 being heatable. The northern part of the building is characterized by these large rooms, whereas the south features the corridors C11a–e. Resistivity mapping shows partly still relatively intact paved floors in these corridors; magnetic data with strong anomalies indicate burnt-brick paving. Corridor C11a along the south side of the building is 3 m wide and gives way to the interior at three points with the corridors C11b–d. These are up to 3 m wide and enclose—with the transversal corridor C11e—two square rooms, each about 120 m^2 in size, being subdivided into further smaller units (C13–C18). Symmetrically to the east and the west two rooms about the same size are also subdivided (C19–C22). The interpretation of theses walls based on geoelectric data has to be hypothetical as debris of the pavement and wall debris cause uncertainties. The halls along the forum are prolonged by rooms C23–C25 and C26–C29. Between C25 and C28 the smaller rooms C29 and C30 are situated as extensions of corridor C11e to the east and west.

Archaeological interpretation of GPR data

At this stage the results can be enhanced by GPR data giving higher resolution and—the most important feature–depth information. Important hints about the mineralogical composition of the layers in the measured area can be found taking a close look at the absorbtion of amplitudes. Table 2 shows the correlation of amplitudes in the subsequent depth ranges, calculated for the whole test area. For interpretation one has to take into consideration that a mean signal attenuation has to be expected with increasing depth independent of the mineralogical composition of the soil. In areas with higher attenuation an increase of highly conductive materials, such as clay, silt and water, can be suspected, whereas less conductive materials such as sand and gravel cause less attenuation. Strong reflective layer interfaces can lead to amplification of the amplitudes. The time slices visualized and used for archaeological interpretation show the summarized amplitude using a range of 0.15 m thickness. The grey scale is defined as light greys giving low amplitudes (strongly absorbing material) and dark shades indicating high amplitudes (strongly reflecting material) accordingly. The single time slices can be combined and interpreted archaeologically as follows (Figures 10–14).

Depth range 0 m to 0.6 m

In Figure 10, depth 0.0–0.30 m, the southern part of the measured area, already grown with crop, can be clearly distinguished from the northern part, covered with a 10 cm layer of snow clearly reducing surface reflections. The diagonal lines on the first four images of Figure 10, depth 0.0–0.60 m, depict the direction of ploughing. The depth range down to 0.6 m can be classified as the Ap horizon. Ploughing depth of down to 0.6 m is quite remarkable but still moderate compared with other areas in Carnuntum. Figure 10, depth 0.45–0.60 m, gives the first traces of debris and upper edges of walls already affected by ploughing and erosion. Owing to the relation of amplitudes of the different levels it can be seen that from 0.45 m onwards the clay layers beyond the humus are affected by the plough (see Table 2). Rooms C15, C18, C20 and C22 clearly show the debris of their southern walls. Room C9 is visible by the debris of all four walls tumbled into its interior.

Depth range 0.6 m to 0.9 m

At this level shadowy contours of the building with rooms C9 and C2 become visible, with debris of C9 sloping into the interior of the room. The top of the north and east wall of room C9 and the west and south walls of C2 as well as parts of the west and south exterior walls can be detected starting at a depth of 0.8 m. In the interior of rooms C15, C18, C20 and C22 wedge shaped layers make the collapsed walls obvious. The rooms seem to be bipartite and down to 0.8 m filled with stony material from collapsed masonry. Room C2 is clearly visible by a clay or humus layer at a depth of 0.9 m, similar results show rooms C3, C4, C23, C26 and C27 still covered partly by debris and gravel down to 0.9 m. In the corridors C11 a conductive layer can be traced at 0.8 m, covering the southern exterior wall in C11. It seems that this layer corresponds to a strong magnetic anomaly, which has been interpreted as brick paved floor. This floor is superimposed on the exterior wall and its appearance at only certain points indicates the corridor C11 as being a porticus along the south front of the building. The exterior carrying wall is thus identical with the south walls of rooms C15, C18, C20 and C22, explaining the massive debris layers in this part of the building.

In the second depth range amplitudes 52% higher than in the first depth range were registered. This phenomenon can be explained by strong reflections at the lower edge of the A_p horizon. Below that humus soil a clayey layer (0.6–0.9 m) is superimposed on a clayey-sandy layer down to 1.95 m. The lowest layer down to 2.25 m is sandy-silty reaching the edge of parent soil, sand and gravel (Table 2).

Depth range 0.9 m to 1.2 m

All of the rooms are now clearly visible so that it can be assumed that the end of the destructive level is reached at this point. Interspaces in the walls may be interpreted as doors. Such a door, giving way into room C23, can be traced in the western exterior wall down to a depth of 1.65 m. The horizon of the ancient floor can be assumed in the layer 0.9 to 1.05 m, showing

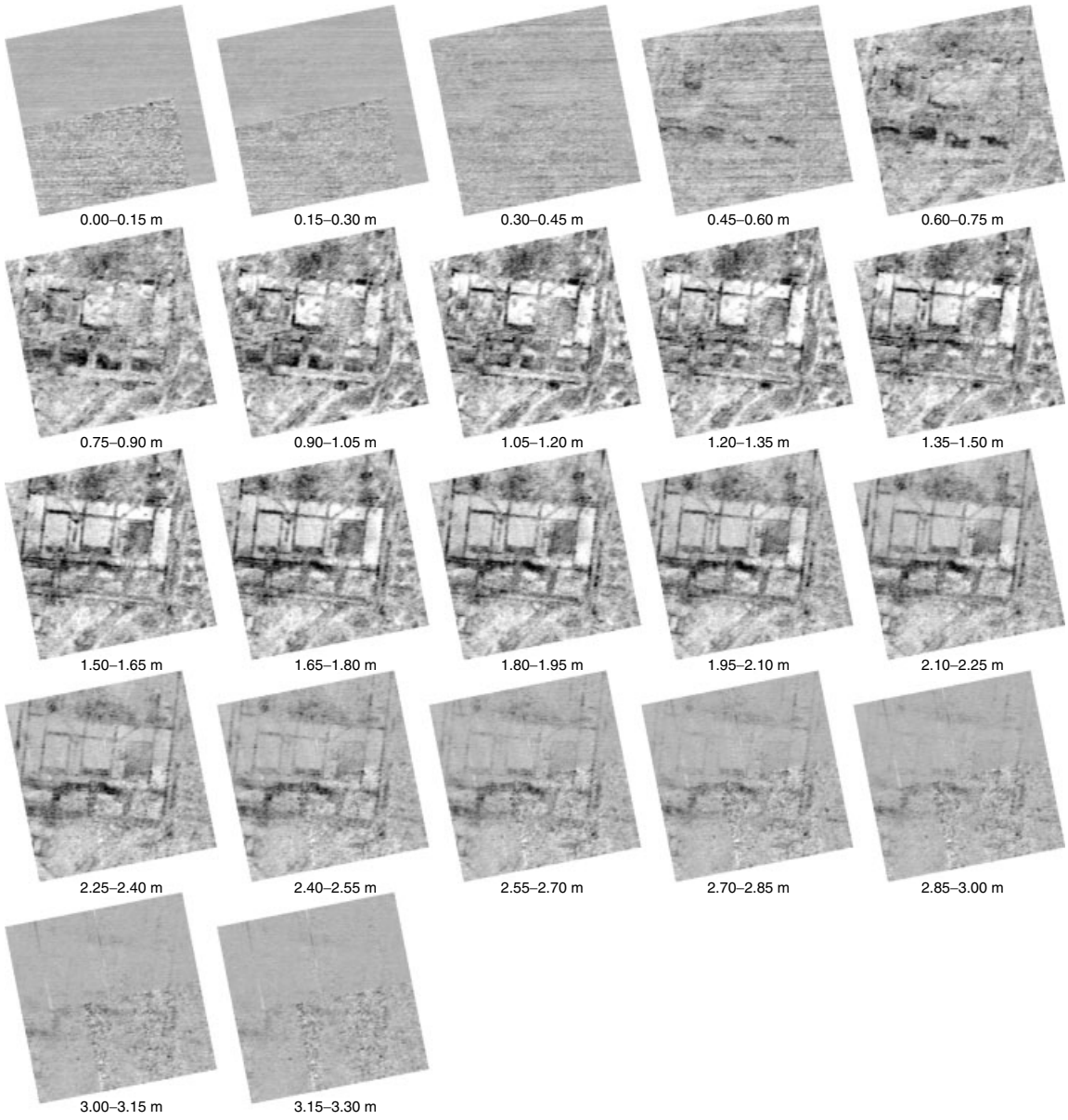

Figure 10. GPR time slices of 3 ns (depth 15 cm). Visualization of the distribution of the absolute amplitude of the reflected radar wave. Areas with high reflection energy are visualized in black.

humus or clay filling in the northern rooms. Faintly visible are the upper edges of the diagonal structures crossing rooms C3 and C4, interpreted as channels or drains. In the northeastern corner of C4 and partly covering the exterior wall a strongly reflecting area of 5×2 m could be detected, possibly another threshold indicating a further entrance leading into room C10. Tracing this anomaly in the animation shows that it runs north and is sloping, thus indicating a staircase leading from the building to the lower levels of the forum. A second staircase was found at the eastern part of the south front at the door leading from corridor/porticus C11a to corridor C11b, the lowest step located at the level of 1.35 m to 1.5 m. The difference in height between the floor of the porticus and the adjoining area is 0.75 m, the staircase being 4 m long. At the western part a

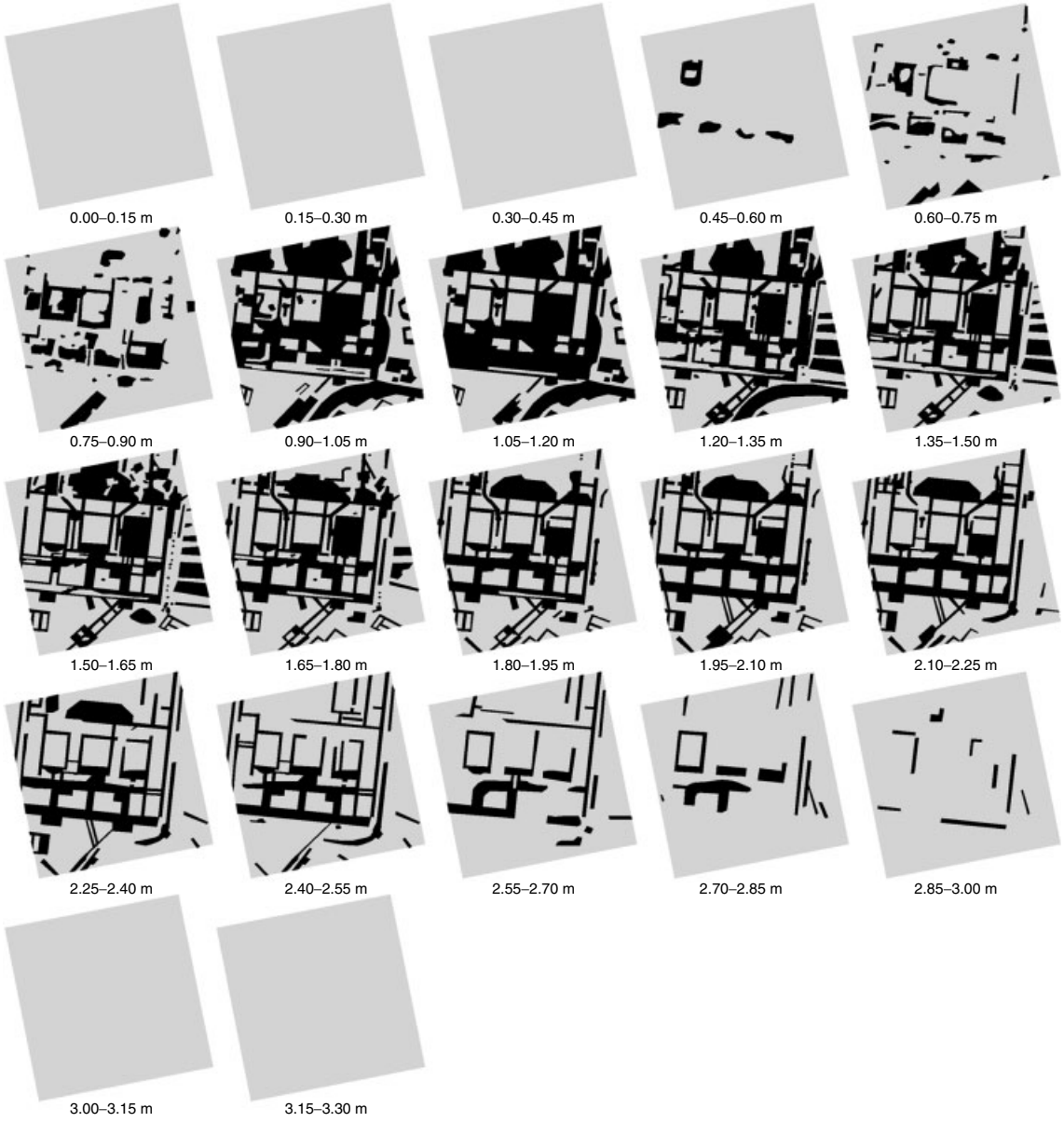

Figure 11. Demarcation of high-reflection areas in the GRP depth slices.

symmetrically arranged staircase leads to a door giving way from porticus C11a to corridor C11d, being discernible at 1.2 m.

Rooms C2, C3, C4, C9, C23, C24, C26 and C27 all show the above-mentioned clay or humus filling, no plastering or gravel can be found. It is very well possible that these rooms had wooden floors. A plastered floor is clearly visible in C10. In the southern part of the building remains of plastering or gravel are traced in the rooms, corridors and portici show plastering. Room C7 reveals an apse at it northern end, positioned right above the end of a channel/drain, possibly indicating a basin. A further porticus seems discernible at the east front. The rooms in the southern part, surrounded by corridors, show subdivisions in the interior by their stratification. The dividing walls could not be traced, but clear

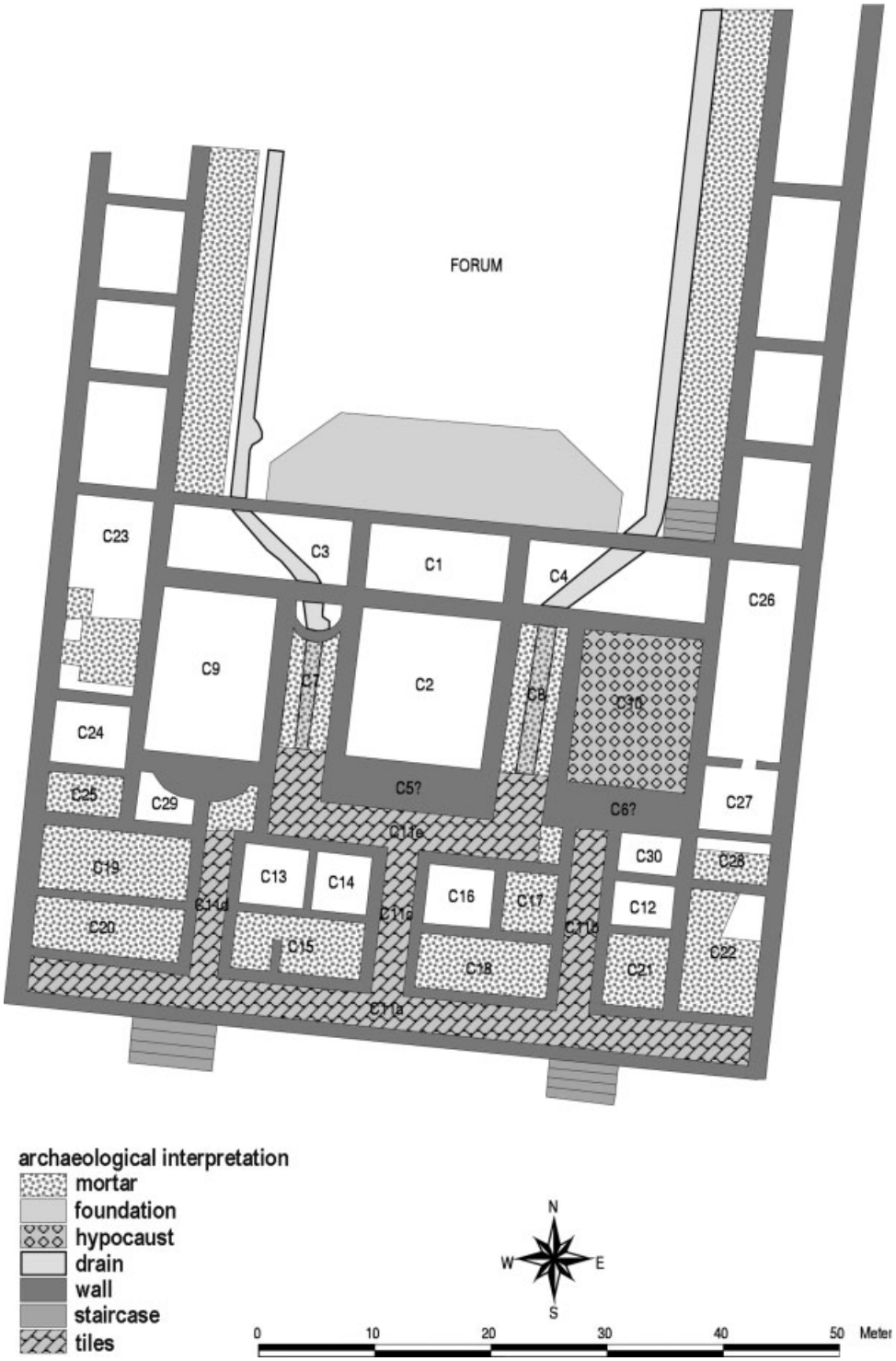

Figure 12. Archaeological interpretation of magnetic, resistivity and GPR survey data with numbering of interpreted rooms.

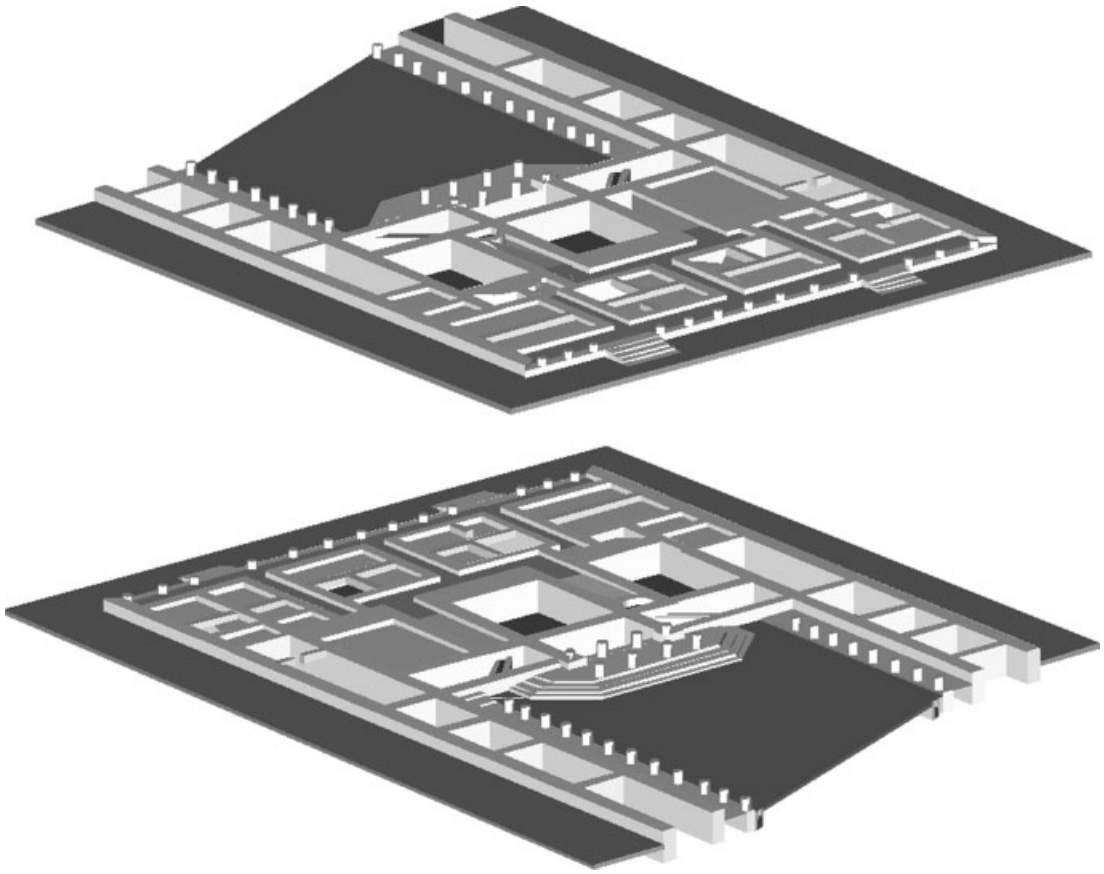

Figure 13. Three-dimensional visualization of the integrated archaeological interpretation.

distinction of areas with different reflections give the conclusive hint. In the following deeper sections the walls become faintly discernible. Small thickness and shallow foundations characterise their non-carrying function. The same layout is found in rooms C23–C25 and C26–C28. The wall dividing C26 from C27 is interrupted, indicating a further threshold at a depth of 1.05 m. A construction with foundations down to 1.65 m at the northern corner of C26 has not yet been interpreted. The large heap of debris at the north front of the building can be traced at a depth of 0.75 m down to 1.2 below the surface, illustrating the different levels of the southern building complex and the open square of the forum.

Depth range 1.2 m to 1.65 m

At this depth, leading below floor level, the walls show up very clearly, fillings or weak substructures are visible but hard to interpret. The above-mentioned rooms with wooden floors indicate slowly increasing percentage of sand and gravel merging with topsoil, the deepest at 2.7 m below surface. In contrast, the northern rooms show clay or humus layers and inhomogeneous material is traced down to 2.4 m. It seems possible that this part was constructed with a cellar level. The corridors are characterized by increasingly sandy layers reaching down to the foundations at some point. The south section of room C9 can be distinguished clearly from the corridor at a depth of 1.2 m, revealing the foundations of an apsis. In room C10, symmetrically arranged but without an apse, the inhomogeneous layers at 1.8 m seem to correspond to the hypocaust system already identified in the magnetogram.

The channels or drains become more visible to the north with increasing depth in single images as well as in the animation. This definite descent supports the interpretation as channels/drains.

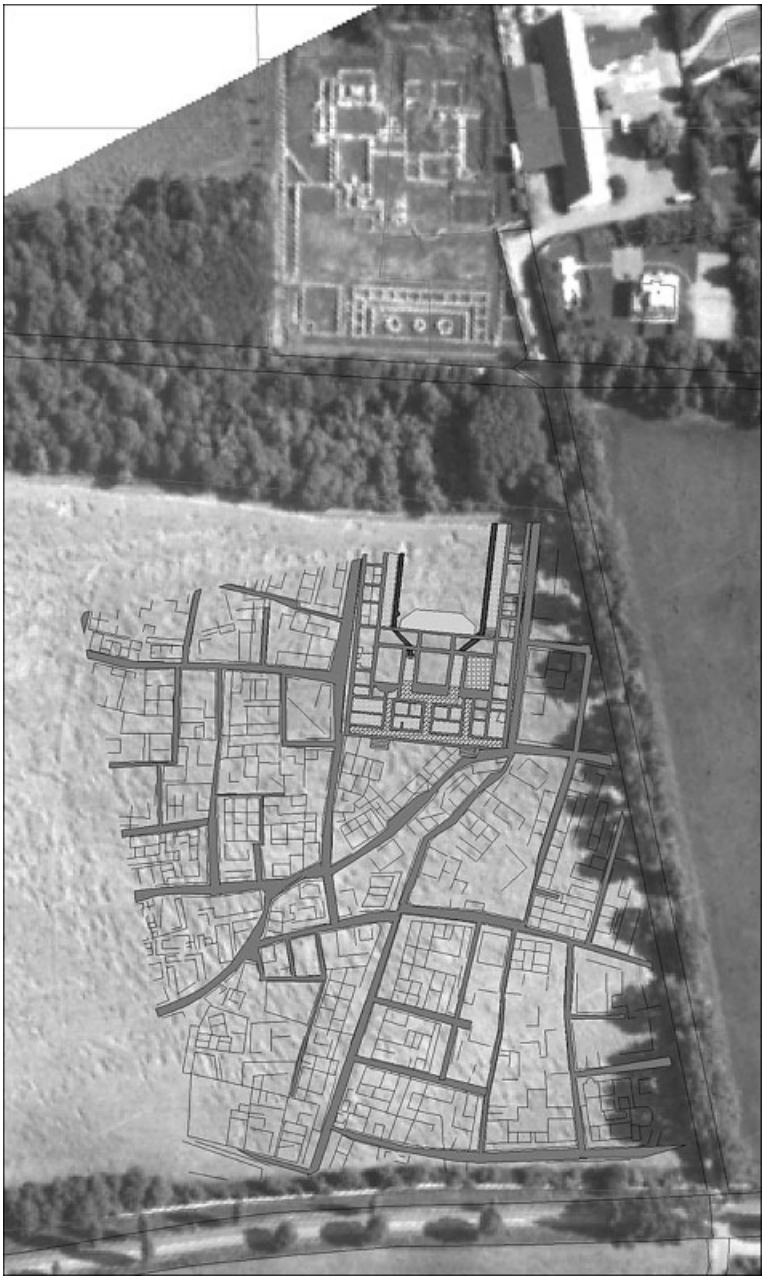

Figure 14. Orthophotograph superimposed with the integrated archaeological interpretation map. Orthophotograph release number: BMLV Nr.: 13.088/12-1.4/00.

Their upper edge in the building lies at floor level, the lower edge at a depth of 1.8 to 1.95 m. In the area of the forum the upper and lower edges can be traced at 1.5 m and 2.25 m respectively. Large, strongly reflecting layers are found at the area of the forum, most evident at a depth of 1.5 m, assumingly representing the ancient street level with stone paving. This layer correlates perfectly with the upper edges of the channels, being probably also covered with stone slabs. The portici opening on to the forum are situated at a level a little higher, identified by remnants of a floor covering of plaster about 50 cm below the large building's floor level and reached by the

previously mentioned staircases at the northern front. From a depth of 1.5 m onwards the outer foundation walls of the portici are traceable. These portici seem to have been reached from the forum by one or two steps. The shops (tabernae) within the east and west halls are visible by debris of their walls. At the east, parallel to the building, at about 1.5 m to 1.8 m depth, are found a row of large stone slabs set in irregular spacing. These could be the covering of a drain running below the street and reaching down to 2.55 m to 2.7 m.

Depth range 1.65 m to 2.1 m

At 1.65 m to 2.1 m the visible structures of room C10 move slowly southward. This fact could indicate sloping layers. The entrance to this room seems to have been from the south as prolongation of corridor C11b, as the elongation of the corridor walls shows at 1.65 m. In front of the entrance hall C1 broad foundations from 1.8 m to 2.25 m have been found, apparently the substructure of a large staircase leading to the forum. The width and the bulkiness of this foundation leads to the conclusion that another porticus or columnaded doorway was erected in front of the entrance. The foundations of the halls bordering the forum are clearly discernible from 1.8 m on. At this depth the floor level has been reached, very possibly starting at 1.35 m. The shops seem to have been equipped with cellars serving as storage rooms, as the foundations reach down to the depth of 2.7 m. The massive walls indicate that the porticoed halls may have had a second floor.

At the same level the channels leading from the interior of the large building in the direction of the River Danube are found again. Running along the portici implies that they served as drains for the rain water collected from the halls' roofs. Another drain is visible to the west of the building reaching from 1.65 m to 2.55 m for the lower edge. This drain is situated under the centre of a road leading northwards along the western side of the building and seems to have a shaft built in, discernible to a depth of 2.25 m.

Depth range 2.1 m to 2.55 m

There seems to be an additional drain at the east side of the building constructed similarly with a shaft where it is bending westwards. This shaft appears to be much larger than the corresponding shaft on the west side. Judging by the dimensions the western shaft could have served as inlet whereas the eastern shaft could be a manhole. The fact that the larger shaft reaches below the floor of the channel and therefore could have served as collecting basin strengthens this theory. The corridors show a layer increasingly mixed with sand and gravel down to the lowest foundation level. The structures joining the south wall of corridor C11e could be massive foundations but also could be debris of tumbled walls of the rooms interpreted as cellars. Features at a depth of 1.95 m to 2.4 m in the rooms C13–C15 and C16–C18 can be identified as basement staircases.

Depth range 2.55 m to 3.3 m

The lower edge of nearly all the walls is reached at 2.55 m, only room C9 still shows up clearly as well as the massive south walls of C5 and C10 and parts of the east wall. Bases of foundations are to be seen under the corridors. From 2.7 m onwards undisturbed gravel layers are registered down to 3.3 m.

Three-dimensional visualization

The archaeological interpretation model derived from the geophysical prospection data can be visualized three-dimensionally and this allows the specialist as well as lay people an easily understandable view of the buried archaeological remnants (Figure 13). On the basis of this interpretation model, computer aided reconstruction can be used for further illustration to a wider audience. By combining archaeological knowledge with architectural construction techniques from the Roman period, we try to derive virtual reality scenes that illustrate a reconstructed scenario of an archaeological site or monument (Hirschegger-Ramser *et al*., 1999). By using software for architectural modelling as well as desktop virtual reality techniques, we create virtual walkthroughs of the roman civil town of Carnuntum. The computer aided reconstruction is a fast and cost effective way to present the archaeological interpretation model derived from prospection data to the public. Computer aided reconstruction of archaeological sites provides a

wide base for archaeological discussion, giving the opportunity for dynamic development of the scene.

Conclusions

The aim of the case study presented here was the development of a standardized combination of geophysical–archaeological prospection methods to create a very detailed interpretation model of archaeological monuments. A large building complex in the civil town of Carnuntum was chosen as the study area. In the resistivity and magnetic images the investigated building complex with a symmetrical layout stand out against the surrounding, heavily built-up district with a complicated street system. The combination of both types of data and their archaeological interpretation resulted in a first interpretation model (Neubauer and Eder-Hinterleitner, 1997). The aim of the subsequent GPR measurements was to gain higher resolution and depth-related information.

The adaptation of a commercially available PulseEKKO 1000 GPR device for archaeological application and the determination of adequate measuring parameters was done by test measurements. The experience showed that the measuring distances conventionally used until 1998 are not appropriate for complex archaeological questions. Line spacing—as for other methods used in archaeological prospection—must not be any larger than 0.5 m. Further, conventional visualizations of single vertical sections are difficult to read and understand. Therefore only a small part of the information in the measuring data has been used so far for interpretation. Archaeological interpretation is thus made difficult or even impossible. The negative feedback from archaeologists, based mainly on the lack of relevant interpretation, hindered the application of this highly informative and totally non-destructive method of prospection. To use GPR in archaeological interpretation, a standardized way of data representation and visualization following the procedure of geomagnetic and resistivity mapping had to be developed. As testing of commercial software had shown no convincing results, adequate software had to be developed enabling us to form a three-dimensional data block of the reflected energy and to produce time or depth slices as digital images in horizontal or vertical directions. Animation of such image sequences makes mental recognition of archaeological structures by the interpreter easier. Digital image sequences found via selection of relevant horizontal depth slices are geo-referenced and integrated in the GIS for subsequent detailed, depth correlated archaeological interpretation. The interpretation drawings derived from GPR-data in combination with the available resistivity and magnetic data as well as information gained from aerial photography lead to a detailed archaeological interpretation model. Two-dimensional interpretation maps and three-dimensional interpretation models can be derived from this basis.

A large building complex with symmetrical layout covering an area of over 3000 m^2 and a wall thickness of up to 1.5 m forming the southern part of the forum of the civil town of Carnuntum was explored. The northern part of the building complex could be reached from the lower open square of the forum by a monumental staircase and shows three large halls of 150 m^2. One of these halls has an apse, the corresponding room to the east is equipped with hypocausts, thus heatable and probably being the curia, the meeting hall of the city council. The central hall shows a pedestal or platform in front of the back wall. In the southern part, small rooms partly constructed with cellars are flanked by corridors. These were reached by two staircases and a porticus from another triangular area in the south. The halls lining the forum, each with a porticus, presumably housed shops with cellars. Below the floor level of the building two channels/drains leading to the River Danube were traced. Beside these important layout features additional information about depth of foundations, filling layers and plastering as well as the height of the remaining walls and the position of wall debris and the penetration depth of modern ploughs could be documented.

Outlook

Experience resulting from this case study and the evaluation and interpretation methods developed, provide the opportunity to plan a specific

strategy for overall prospection of Carnuntum. Such a prospection seems to be urgently necessary from the scientific as well as from the development-planning point of view and could give enormous input to economic strategies by coordinated and focused action for the largest archaeological zone in Austria. As a first consequence a follow-up project for further development of GPR methodology and its application to cover the entire insula of the forum and the adjacent decumanus maximus was granted by the Ministry of Science and will be finished in 2001 (Kandler *et al*., 2001).

Acknowledgements

The authors wish to thank Angela Schwab for fruitful discussion and review of the paper and Michael Doneus for making the digital orthophotograph in Figures 1, 9 and 14 available. Geophysical field work was carried out by Archeo Prospections® of the Central Institute for Meteorology and Geodynamics, Vienna. We would like to thank Erol Bayirli and Michael Duma for helping with field work. The georadar survey was sponsored by the Austrian Ministry of Science and Traffic, project number 30.649/1-III/2/97.

References

Becker H. 1985. Verarbeitung magnetischer Prospektionsmessungen als digitales Bild. *Das Archäologische Jahr in Bayern* **1984**: 184–186.

Becker H. 1995. From nanotesla to picotesla—a new window for magnetic prospecting in archaeology. *Archaeological Prospection* **2**: 217–228.

Clark A. 1990. Seeing beneath the soil. Batsford: London.

Conyers LB, Goodman D. 1997. *Ground Penetrating Radar. An Introduction for Archaeologists*. Altamira Press: Walnut Creek.

Doneus M, Neubauer W. 1997. Two-dimensional combination of prospection data. *Archaeological Prospection* **5**: 29–56.

Doneus M, Neubauer W, Scharrer G. 2001. Arcghäologische Prospektion der Landschaft von Carnuntum-Möglichkeiten der Luftbildarchäologie. *Carnuntum Jahrbuch* **2000**: 53–72.

Goodman D. 1994. Ground penetrating radar simulation in engineering and archaeology. *Geophysics* **59**(2): 224–232.

Goodman D, Nishimura Y, Rogers JD. 1995. GPR time slices in archaeological prospection. *Archaeological Prospection* **2**: 85–89.

Hirschegger-Ramser P, Ferschin P, Kandler M, Neubauer W. 1999. Computer aided virtual reality reconstruction based on prospection data. An example from the Roman town Carnuntum/Austria. *Arbeitshefte des Bayerischen Landesamtes für Denkmalpflege* **Band 108**: 41–42.

Jobst W. 1983. *Provinzhauptstadt Carnuntum*. Österreichs größte archäologische Landschaft: Wien.

Kandler M, Neubauer W, Seren S, Eder-Hinterleitner A. 2001. The forum of the civil town of Carnuntum and its surroundings. In *Archaeological Prospection*, Doneus M, Eder-Hinterleitner A, Neubauer W (eds). Fourth International Conference on Archaeological Prospection, Vienna: 120–123.

Lorra S. 1996. Geophysikalische Prospektion und Modellierung archäologischer Fundplätze in Schleswig-Holstein. *Universitätsforschungen zur Prähistorischen Archäologie* **Band 36**: 1 pp.

Malagodi S, Orlando L, Piro S, Rosso F. 1996. Location of archaeological structures using GPR method: three-dimensional data acquisition and radar signal processing. *Archaeological Prospection* **3**: 13–23.

McCann WA. 1995. GPR and archaeology in central London. *Archaeological Prospection* **2**: 155–166.

Neubauer W. 1990. Geophysikalische Prospektion in der Archäologie. *Mitteilungen der Anthropologischen Gesellschaft in Wien* **120**: 1–60.

Neubauer W. 2001a. Images of the invisible-prospection methods for the documentation of threatened archaeological sites. *Naturwissenschaften* **88**: 13–24.

Neubauer W. 2001b. Magnetische Prospektion in der Archäologie. *Mitteilungen der Prähistorischen Kommission* **44**: Österreichische Akademìe der Wìssenschaften: Wìen.

Neubauer W, Eder-Hinterleitner A. 1997. Resistivity and magnetics of the Roman town Carnuntum, Austria: an example of combined interpretation of prospection data. *Archaeological Prospection* **4**: 179–189.

Neubauer W, Melichar P, Eder-Hinterleitner A. 1996. Collection, visualization and simulation of magnetic prospection data. *Analecta Praehistorica Leidensia* **28**: 121–129.

Neubauer W, Eder-Hinterleitner A, Melichar P, Steiner R. In press. Improvements in high resolution archaeological magnetometry. *Prospezioni Archeologiche*.

Scollar I, Weidner B, Segeth K. 1986. Display of archaeological magnetic data. *Geophysics* **51**: 623–633.

Walker AR. 2000. Multiplexed resisitivity survey at the Roman town of Wroxeter. *Archaeological Prospection* **7**: 119–132.

